



Review

MXene Based Nanocomposites for Recent Solar Energy Technologies

T. F. Alhamada ^{1,2}, M. A. Azmah Hanim ^{2,3,*}, D. W. Jung ^{4,*}, R. Saidur ⁵, A. Nuraini ² and W. Z. Wan Hasan ⁶

¹ Department of Scientific Affairs, Northern Technical University, Mosul 41001, Iraq

² Department of Mechanical and Manufacturing Engineering, Faculty of Engineering, Universiti Putra Malaysia, Serdang 43400, Selangor, Malaysia

³ Advance Engineering Materials and Composites Research Center (AEMC), Faculty of Engineering, Universiti Putra Malaysia, Serdang 43400, Selangor, Malaysia

⁴ Department of Mechanical Engineering, Jeju National University, 1 Ara 1-dong, Jeju 690-756, Korea

⁵ Centre for Nano-Materials and Energy Technology (RCNMET), School of Engineering and Technology, Sunway University, Petaling Jaya 47500, Selangor, Malaysia

⁶ Department of Electrical and Electronic Engineering, Faculty of Engineering, UPM, Serdang 43400, Selangor, Malaysia

* Correspondence: azmah@upm.edu.my (M.A.A.H.); jungdw77@naver.com (D.W.J.)

Abstract: This article discusses the design and preparation of a modified MXene-based nanocomposite for increasing the power conversion efficiency and long-term stability of perovskite solar cells. The MXene family of materials among 2D nanomaterials has shown considerable promise in enhancing solar cell performance because of their remarkable surface-enhanced characteristics. Firstly, there are a variety of approaches to making MXene-reinforced composites, from solution mixing to powder metallurgy. In addition, their outstanding features, including high electrical conductivity, Young's modulus, and distinctive shape, make them very advantageous for composite synthesis. In contrast, its excellent chemical stability, electronic conductivity, tunable band gaps, and ion intercalation make it a promising contender for various applications. Photovoltaic devices, which turn sunlight into electricity, are an exciting new area of research for sustainable power. Based on an analysis of recent articles, the hydro-thermal method has been widely used for synthesizing MXene-based nanocomposites because of the easiness of fabrication and low cost. Finally, we identify new perspectives for adjusting the performance of MXene for various nanocomposites by controlling the composition of the two-dimensional transition metal MXene phase.

Keywords: MXenes; nanocomposites; solar cells; power conversion efficiency



Citation: Alhamada, T.F.; Azmah Hanim, M.A.; Jung, D.W.; Saidur, R.; Nuraini, A.; Hasan, W.Z.W. MXene Based Nanocomposites for Recent Solar Energy Technologies. *Nanomaterials* **2022**, *12*, 3666. <https://doi.org/10.3390/nano12203666>

Academic Editor: Baizeng Fang

Received: 15 September 2022

Accepted: 12 October 2022

Published: 18 October 2022

Publisher's Note: MDPI stays neutral with regard to jurisdictional claims in published maps and institutional affiliations.



Copyright: © 2022 by the authors. Licensee MDPI, Basel, Switzerland. This article is an open access article distributed under the terms and conditions of the Creative Commons Attribution (CC BY) license (<https://creativecommons.org/licenses/by/4.0/>).

1. Introduction

Scientists have opened the floodgates to researching clean, renewable energy in the past few years. They think solar energy is the most abundant energy source that can meet society's needs, which come from economic growth [1]. Solar energy can be used for everything from heating water to generating electricity. Solar energy can be harvested using photovoltaic (PV) technology. Reports on the world's solar photovoltaic electricity supplies say that PV technologies will provide around 345 GW and 1081 GW by 2020 and 2030, respectively [2,3]. Southern European countries have found solar energy to be the most cost-effective option available. The analysis's resolution was set at the regional level. Sustainable development advocates often cite the importance of integrated renewables like building-integrated photovoltaics [4]. A technical-economic study has been conducted by Ali and Alomar to evaluate the productivity of grid-connected photovoltaic (PV) solar systems. This study proved that investment in the technology of PV systems is quite favourable [5].

Research of nanomaterials is currently at the forefront because of its potential to solve issues crucial to human existence in areas like the environment, energy, medicine, fuel,

etc., [6]. For nanomaterials, zero-dimensional, one-dimensional, and two-dimensional classifications exist. Combining nanoparticles with other bulk materials can also generate three-dimensional nanomaterials. Numerous studies have shown that 2D nanomaterials are very important. Two-dimensional nanomaterials can also be used in optoelectronic devices because of their capacity to modify their optical characteristics through their thickness [7,8].

In 2011, Gogotsi et al. investigated transition-metal nitrides, or carbides (MXenes), as star materials from MAX phases, which are layered compounds similar to graphite with monoatomic A-element layers sandwiched between metallic electrically conductive and stiff MX-blocks. The new compound was called MXenes because the A element had been removed from the MAX phase and its structure was similar to graphene [9].

Commercialization of perovskite solar cells requires high efficiency and excellent stability. According to the work of Bati et al., functionalizing MXene nanosheets with cesium ions and incorporating them into the perovskite layer can result in devices with improved efficiency and increased thermal stability. Passivating perovskite defects using additive, interface, and compositional engineering has been accomplished to date [10,11].

Guo et al. achieved a 12% increase in efficiency by adding MXene to the perovskite precursor [12]. Agresti et al. later demonstrated that MXene could boost PSC PCE by 26% and reduce hysteresis when used as a dopant or interlayer. According to these conclusions, MXenes have the potential to serve as dopants in PSCs [13,14].

In order to better understand the physics and chemistry behind them, MXene-based materials for solar cell applications are categorized into various roles, including as electrodes, additives in perovskite solar cells, electron/hole transport layers, and MXene-silicon based heterojunction solar cells [15,16]. When MXenes are used in perovskite solar cells, the ion transport speed increases and the crystalline size is extended, which benefits energy conversion [8]. The solar cell properties of functional nanomaterials, such as 2D materials like MXene, are far superior to those of traditional materials. Energy conversion efficiency has been measured at 26.5%, three times greater than carbon nanotube silicon photovoltaic cells. Photovoltaics research has focused on 2D layered nanomaterials because of their unique properties. The complex roles that MXenes play in solar cell designs have been the biggest obstacle to their widespread use [17].

MXenes are a viable option for use in a wide variety of settings due to their adaptability and appealing characteristics. Its outstanding features, including high electrical conductivity, Young's modulus, and distinctive morphology, make it very advantageous for composite construction [15]. Photovoltaic systems that turn solar energy into electrical energy have a promising future as a clean energy source due to the material's good electronic conductivity, ion intercalation, chemical stability, and tunable band gaps. For photovoltaic conversion, nanostructured devices have evolved from the original wafer-based devices. These devices take advantage of a distributed heterojunction to produce and transfer charges in spatially separated phases. In most photovoltaic cells, two materials are used to separate the electron-hole pairs and charge transfers that lead to photocurrent generation [18]. Work functions for MXenes range from as low as 2.14 electronvolts to as high as 45.65 electronvolts. It was found that the work function was highly dependent upon the functional groups present on the surface, with the presence of $-O$ groups increasing the work function and the presence of $-OH$ groups decreasing it. When the barrier height is changed to an appropriate range for semiconductors or metal contacts, photocurrent can be generated [19]. A MXene-Si Schottky junction cell was fabricated by maintaining MXene and Si in contact with one another in a vertical van der Waals heterostructure. This cell had an open voltage of 0.34 V and a current density of 12.9 mA cm^{-2} under 100 mW cm^{-1} . Strain engineering semiconductors could achieve excellent photoelectronic applications. A MXene-blue phosphorene heterojunction, for example, exhibits a valence band minimum from MXene and a conduction band minimum from phosphorene under conditions of moderate strain. In contrast, as the strain is increased, the band alignment is flipped. This heterostructured junction material will significantly benefit the development of photoelectronic and novel photonic applications [20]. For more than 1900 h, Chen et al. produced a

solar cell with a high incipient power conversion efficiency of around 9.01% and long-term stability [18]. This electron is then transferred to a carbon electrode via a perovskite film, where it accumulates and is discharged through holes in the perovskite film. As shown in Figure 1, the charge transport arrangement and mechanics are depicted [21,22].

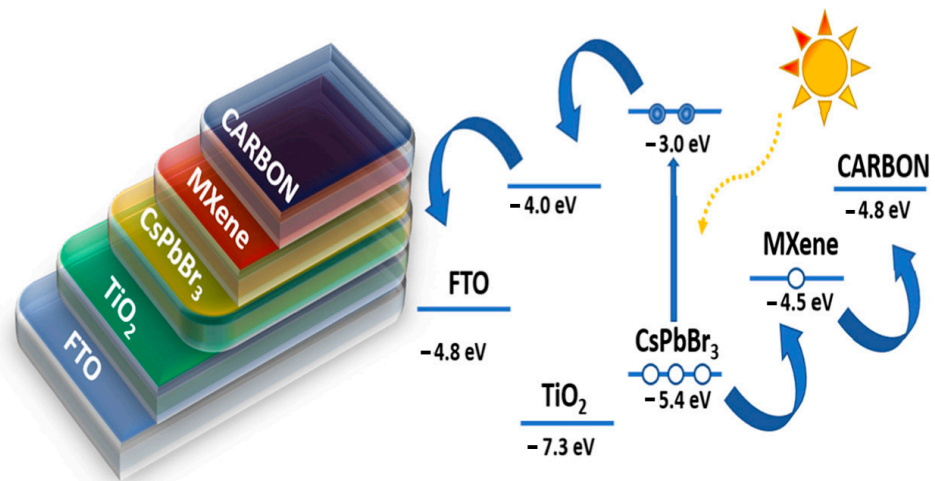


Figure 1. Shows the structure and charge transport mechanism of an FTO/TiO₂/CsPbBr₃/Ti₃C₂-MXene/carbon perovskite solar cell. Reprinted with permission from Ref. [22]. 2021, Elsevier.

In recent years, the efficiency of power conversion in perovskite solar cells (PSCs) has continued to rise, attracting researchers' interest [23]. First, Nb₂C MXenes were introduced as an external addition to the SnO₂ electron transfer layer (ETL) developed by Y. Niu et al., which led to a noticeable growth of SnO₂ grains, as shown in Figure 2. They obtained a maximum power conversion efficiency of 22.86%, and these target devices maintained 98% of their initial efficiencies after 40 days at 25 degrees Celsius and 40–60 percent humidity [24].

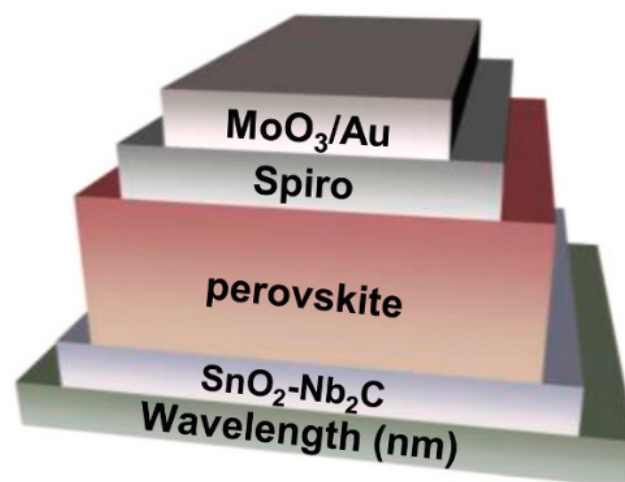


Figure 2. Schematic of the PSCs structure. Reprinted with permission from Ref. [24]. 2021, Elsevier.

The main objective of this paper was to describe in detail the fundamental principles for creating each 2D transition metal MXene structure-based nanocomposite and its tunable properties depending on the composition of transition metals. We offer an alternative approach to obtaining efficient PSCs by providing an in-depth mechanistic understanding of MXene interface engineering. Figure 3 shows a schematic overview of the different

MXene NCPs discussed in this review paper, such as MXene-polymer, MXene-metal oxide, and MXene-carbon.

This paper summarizes all the documented work on incorporating MXene-based nanocomposites into recent solar energy technologies to enhance solar power generation and work stability. The following section describes perovskite-based solar cells. Section 3: Fabrication of MXene-nanocomposite and enumerates the many functions performed by MXene in solar cells. After that, the role of MXene surface termination groups. Section 5: MXene-based nanocomposites and how they are classified. A conclusion and prospects are given in Section 6.

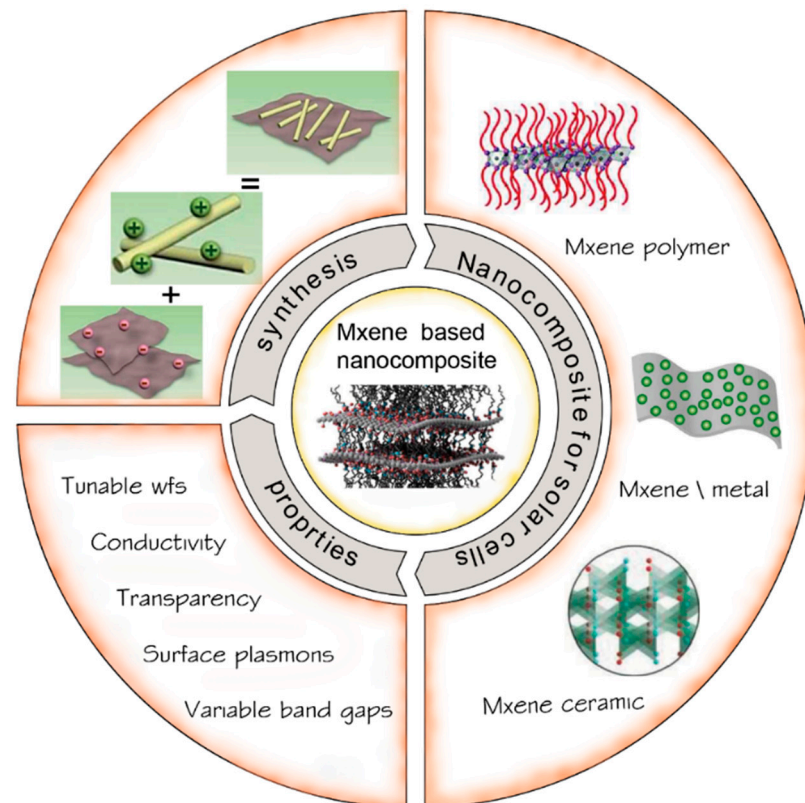


Figure 3. An illustration of a schematic overview of MXene-based nanocomposites for solar cell applications.

2. Perovskite-Based Solar Cells

Since PVS solar cells have such good light-harvesting qualities, they have developed rapidly in recent years, and numerous milestones have been attained in this sector, such as a high PCE of up to 23.2%, stability for more than a thousand hours, and so on. However, in order to meet its potential PCE limits (30–33%), a number of complex difficulties, such as the higher crystal size and fewer grain boundaries, must be handled. Two-dimensional MXene ($\text{Ti}_3\text{C}_2\text{T}_x$) was initially suggested as an additive in PVS solar cells by Guo et al. in their paper [12,25–28]. Inserting a Ti_3C_2 -MXene has an energy level that is higher than the carbon electrode, which lowers PVS's conduction and valence band, thereby decreasing the pace at which the photocurrent is transferred and accelerating the transfer of the hole, which is represented in Figure 4a [21]. By inserting a thin layer of Ti_3C_2 -MXene, it is possible to passivate the PVS flake surface and create a direct conducting channel between Ti_3C_2 -MXene and CsPbBr_3 , which speeds up carrier transport to the carbon electrode. Recently, 2D Ruddlesden–Popper PVS solar cells have been suggested as a way to improve the long-term stability of operation. Jin et al. [29] demonstrated perovskite solar cells with $\text{Ti}_3\text{C}_2\text{T}_x$ MXene-doped PVS flakes, which increased the device's current density. In

addition, a MXene-MAPbBr₃ heterojunction is formed using the in situ solution growth method. As shown in Figure 4b,c, the MXene-MAPbBr₃ heterojunction's charge and energy transfer speeds are significantly facilitated, positively contributing to the performance enhancement [30,31].

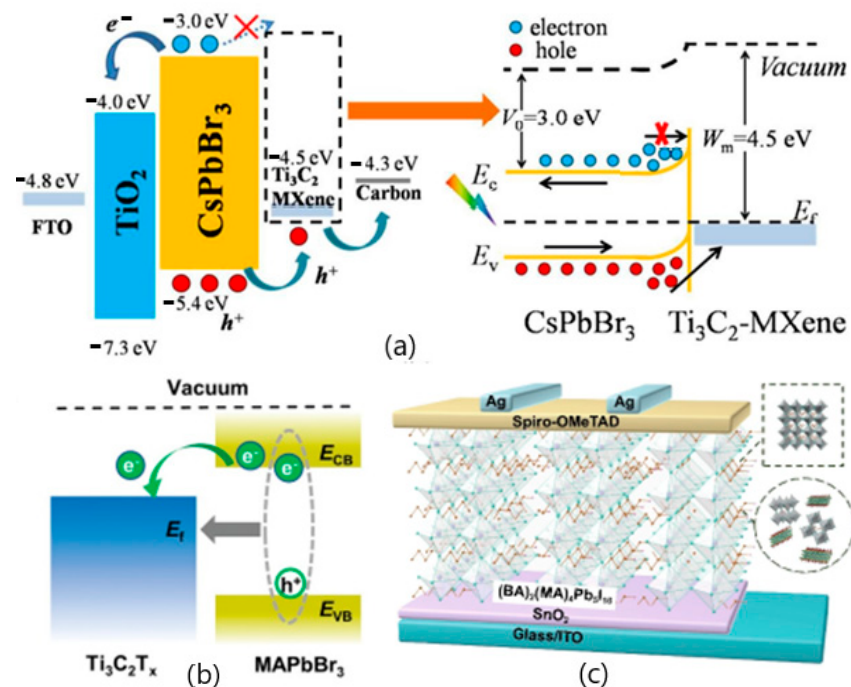


Figure 4. (a) The device's energy bandgap and carrier transport mechanism under illumination at the interface, respectively. Reprinted with permission from Ref. [21]. 2019, Royal Society of Chemistry. (b) Energy transfer scheme between MXene and perovskite nanoflakes. Reprinted with permission from Ref. [29] 2021, Springer Nature. (c) The schematic diagram of the device. Reprinted with permission from Ref. [30]. 2020, John Wiley and Sons.

3. Fabrication of MXene Composite

Composites reinforced with MXene can be made in various ways, from solution mixing to powder metallurgy. MXene composites can be prepared using various methods, some of which are described below.

3.1. Solution Mixing

Solution mixing techniques have produced most MXene-reinforced polymer nanocomposites due to the hydrophilic character of MXene nanosheets supplied by the functional groups [32,33]. As shown in Figure 5, MXene nanoparticles are often distributed in polar solvents such as water [34], *N,N*-dimethylformamide (DMF) [35], and dimethylsulfoxide (DMSO) [36]. Due to their mutual solubility, polymer components might potentially be dissolved in the same dispersant or a different one [35]. These solutions, which consist of the polymer and MXene, are combined and blended to produce a homogeneous slurry of MXene composites. It should be emphasized that the solubility of MXene in nonpolar polymers or those with weakly polar groups is still problematic; thus, a proper surface pre-treatment is required to improve dispersibility [37,38]. Solution mixing is a straightforward procedure that takes advantage of the hydrophilicity of MXene nanoparticles, but serious limitations, such as the formation of an abnormal quantity of environmental waste, poor mechanical qualities associated with the resulting composites, and laborious evaporation of solvents, generally prohibit its application [39].

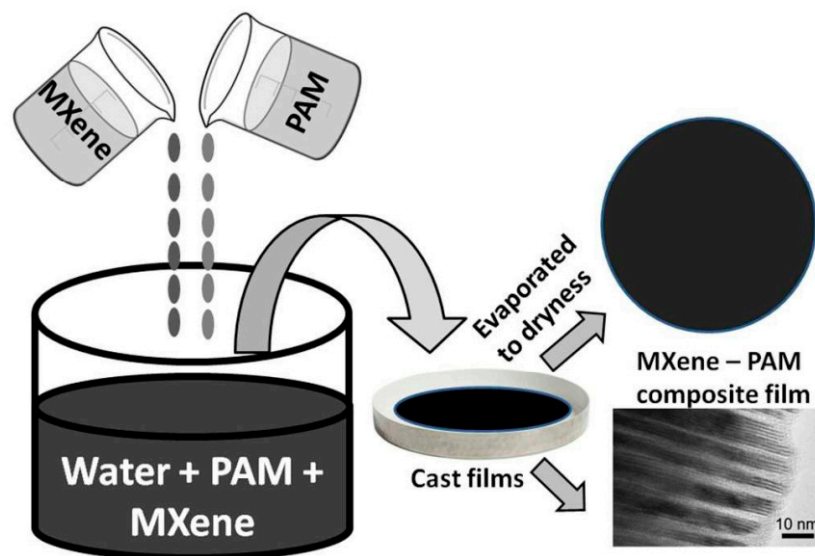


Figure 5. Schematic of the synthesis of MXene-Polyacrylamide nanocomposite films by the solution mixing method. Reprinted with permission from Ref. [40]. 2016, RSC Publishing.

3.2. Hydrothermal Process

The hydrothermal technique, also known as solvent thermal or solvothermal, is an often-documented procedure for producing a variety of new substances, new materials, and new compounds [41–45], especially MXene ceramic nanocomposites because of its simplicity, low cost, and widespread use. As shown in Figure 6, the amount of restacking required by this approach is low, and the resulting distributional uniformity is adequate [46–49]. For instance, BiFeO_3 (BFO)/ Ti_3C_2 nanohybrid was produced by using a straightforward and cheap double solvent solvothermal process for the break-down of organic dye and colourless contaminants [47]. In another study, tetrabutyl titanate $\text{Ti}(\text{OBU})_4$ was used in a straightforward hydrothermal process at a low temperature to create a $\text{Ti}_3\text{C}_2/\text{TiO}_2$ composite [50]. High oxidation or interdiffusion is unavoidable due to the method's use of excessive temperatures, and achieving a uniform dispersion of particles is difficult in comparison to other techniques [51,52].

The significant rise in PCE value is primarily attributable to the synergistic effects of the hydrothermal method and the one-of-a-kind layered morphology of conductive MXene nanosheets and their cocatalysts with CoS nanoparticles. These two factors contribute to the catalytic activity of the material. According to the findings of Chen et al., MXene-based composite CE materials show a great deal of promise for high electro-catalytic activity in QDSCs. These materials generate an abundant number of catalytic active sites, have good permeability, and exhibit outstanding charge transfer and ion-diffusion performance [53].

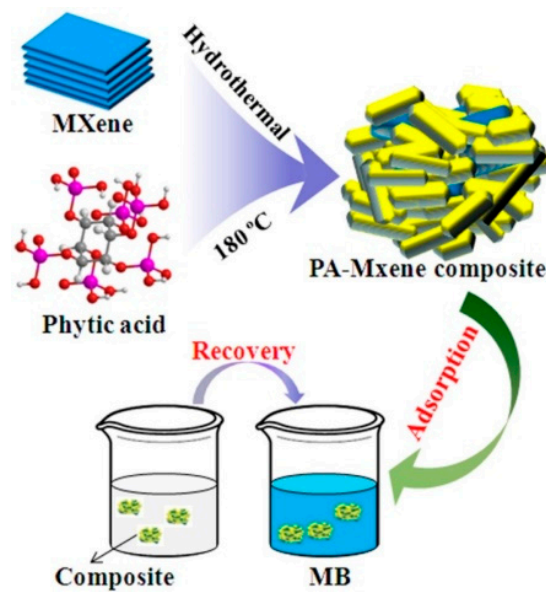


Figure 6. Schematic illustration of Mxene-based composites synthesized via the hydrothermal process. Reprinted with permission from Ref. [54]. 2020, Elsevier.

3.3. Powder Metallurgy

Powder metallurgy reduces waste, makes smooth surfaces, and the process produces less than 3% scrap. Tooling expenses, on the other hand, may be justified in large-scale manufacturing, as shown in Figure 7 [37,55]. An aluminum (Al) matrix containing 10% $Ti_3C_2T_x$ in a polypropylene container was tested for chemical stability using powder metallurgy [56]. After cold pressing, the pellet was sintered without applying pressure at a temperature between 500 and 7001 degrees Celsius [56]. Pressureless sintering followed by a hot extrusion technique was used by [57] to generate $Ti_3C_2T_x/Al$ with a MXene concentration of 0–3 wt%, while [37] used spark plasma sintering to produce $Cu/Ti_3C_2T_x$ with improved tribological characteristics. Self-lubricating Ti_3C_2 nanosheet/copper (Ti_3C_2/Cu) composite coatings were studied by [58], who used an electrodeposition approach at room temperature to create the coatings using Ti_3C_2 nanosheets. Similarly, Refs. [58,59] developed a novel MXene-Ag nanowire composite using a simple electrodeposition approach [52].



Figure 7. Schematic illustration of the powder metallurgy process. Reprinted with permission from Ref. [54]. 2020, Elsevier.

4. Role of Surface Termination Groups

MXenes cleared the way for the possible construction of innovative optoelectronic devices based on developing surface termination groups. Surface termination groups may adjust the band gap without altering the Ti_2CT_x MXene's original structure, and this is a valuable technique for regulating the material's electrical characteristics [60,61]. On the other hand, theoretical investigations have shown that surface termination groups affect the electronic structure of Ti_2CO_2 [62]. The pristine MXenes (Ti_3C_2) have a metallic structure. In contrast, $Ti_3C_2(OH)_2$ terminated with $-OH$ displays semiconducting properties [63]. As a result, surface functional groups ($-OH$ and $-F$) show semiconducting behavior with a valence band–conduction band energy differential of 0.05–0.1 eV [20]. Enyashin et al. theorized that the band gap of $-OH$ terminated Ti_3C_2 within the range of 0–0.042 eV [64]. While the work function of $-O$ and $-OH$ terminated Ti_3C_2 MXenes was shown by Schultz et al. [65]. According to the researchers, the kind of OH termination has little effect on the variations of strain energies in titanium carbide TiC_x nanotubes, but it does affect the relative stability of the planar parent phases, as shown in Figure 8 [64].

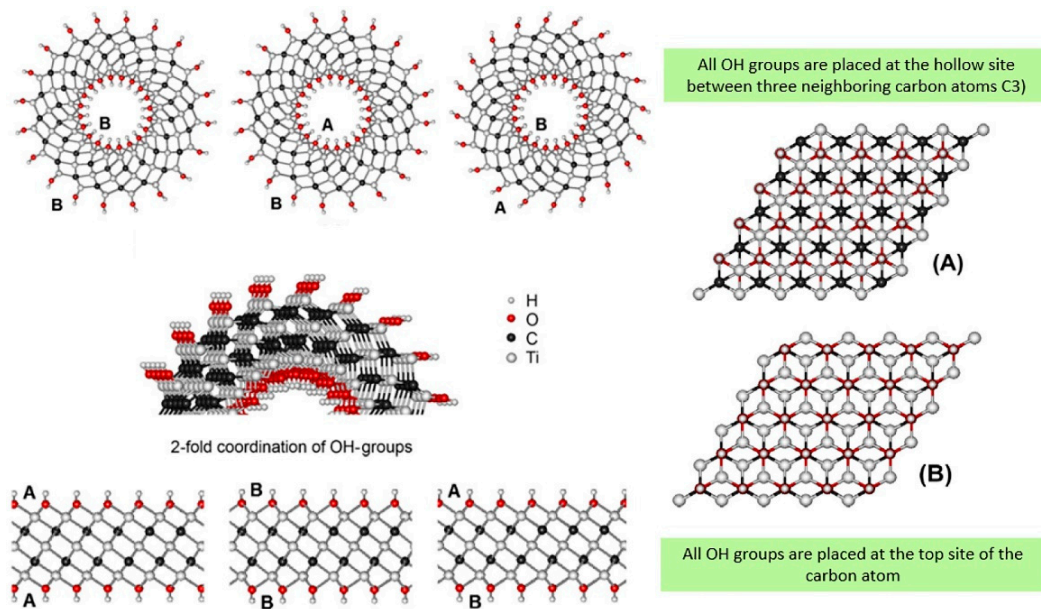


Figure 8. The arrangement of $-OH$ termination at positions (A,B) in the inner and outer walls of $Ti_3C_2T_x$ MXene nanotubes. Reprinted with permission from Ref. [64]. 2012, Elsevier.

Controlling the amount of TiO_2 and Ti_3C_2 in the resulting TiO_2/Ti_3C_2 composite affects the separation of charge carriers based on: (i) the surface alkalization processes of pure Ti_3C_2 ; (ii) hydrothermal oxidation temperature; (iii) calcination temperature; (iv) surface termination groups ($-F$, $-OH$, or $-O$); and (v) hydrothermal reaction time [66]. The chemically reactive M-A bonding in the $M_{n+1}AX_n$ phase makes selective etching of the interleaved A element a viable option for separating $M_{n+1}AX_n$ layers. In 2011, Naguib et al., used a Ti_3AlC_2 MAX phase powder to investigate Ti_3C_2 MXenes (graphene-like morphology) [9].

5. MXene-Reinforced Nanocomposites

Combining MXenes with polymers, ceramics, metals, and nanoparticles yields composites with improved performance. Their exceptional optical, electrical, structural, mechanical, and thermal qualities result from their one-of-a-kind chemical and physical properties. Many other nanomaterials, including graphene derivatives, metal oxides, metals, and polymer monomers, have been successfully merged with MXene to create MXene-based hybrid nanocomposites, which improve upon the characteristics and practicality of pure MXene. Effective types for preparing MXene composites are as follows.

5.1. MXene-Metals/Ceramics Composite

MXenes are often employed to reinforce polymeric materials, but they can also be utilized to reinforce metallic or ceramic materials [67–69]. Reinforcement agents like graphene and CNTs have previously been tried in metals. On the other hand, metal matrix composites have faced significant difficulties due to agglomeration and poor wettability [70]. Pure MXene has been successfully combined with a wide range of nanomaterials, including graphene derivatives, metal oxides, and metals, to create MXene-based hybrid nanocomposites [39].

5.2. MXene-Polymer Composite

Using MXenes, polymer-based composites get a significant advantage in mechanical performance [39,71,72]. MXenes offer a wide range of applications as composite components because of their unique chemistry [16,73,74]. MXenes could greatly affect how spherulites grow and how polymeric materials crystallize [75,76]. Since the MXene sheets have a high aspect ratio and the -OH termination groups provide hydrogen-bonding interactions, the $Ti_3C_2T_x$ was found to significantly alter the glass transition temperature (T_g), and the mechanical strength increased by 23 percent, from 104.6 MPa for pure Nafion to 128.4 MPa for the composite sample [77]. Polymeric molecules respond better to MXene's functional groups than to Graphene's. These functional groups include the $-O_2$, $-OH$, and $-F$. Graphene devoid of surface terminations is often insufficient for composite production [78]. Due to its hydrophilic nature, MXene sheets have excellent wettability with a broad range of materials. It makes it easy to disperse and spread the sheets in various liquids [79]. Currently, MXenes have been employed in several types of polymeric matrices, including polyurethane (PU) [71,80], polyacrylic acid (PAA) [81], polylactic acid (PLA) [16], poly-vinyl alcohol (PVA) [82], nylon-6 [83], chitosan [84], and polyvinylidene fluoride (PVDF) [35], etc.

6. Conclusions and Prospect

Technological development has come a long way since MXene's discovery in 2011. In 2018, two-dimensional transition metal (MXene) contributed to the enhancement of solar cell manufacture by increasing the efficiency of produced energy and solar cells' durability. MXene-based nanocomposites offer incredibly promising possibilities as a future for this remarkably fast-growing subject of nanotechnology and may be further investigated in many fields of science and technology. Substantial work is necessary to characterize and improve the characteristics of MXene-based nanocomposites, resulting in materials with superior desirable features. Even though many MXene-polymer composites are synthesized, understanding how the microstructural characteristics of MXene-metal or ceramic composites influence their physical properties is still in its early stages. More research is required on how varying the concentration of a surface passivating functional group affects its properties. While several MXenes are readily accessible, $Ti_3C_2T_x$ is now the most popular MXene used in solar cell fabrication. This paper reviews the recent progress in MXene-reinforced composites ranging from polymer-based materials to ceramic-or metal-matrix nanocomposites. We summarized the comprehensive studies on using MXene-based nanocomposites in solar cells and collated nearly all the results in the literature, as it has only been four years since MXene's initial application in a solar cell was proven. More research is required on how varying the concentration of a surface passivating functional group affects its properties. The essential device parameters are listed in Tables S1–S3 (Supplemental Data) [85–100].

In light of the above, the essential findings of this study are:

- MXenes interact with other materials to generate hybrids and nanocomposites with enhanced or extra properties. Applications for these novel materials in renewable energy, energy storage, and energy conversion are possible;
- As shown in Tables S1–S3, MXenes, metal oxides, and noble metals have an impact on the device characterization data of solar cells. MXene has been used as a booster in nanocom-

posite for solar cells, which has dominated scientific research because conventionally designed PSCs are more efficient than metal oxide and noble metals;

- Incorporating 2D transition-metal MXenes into the category of 2D materials has improved the design choices for nanomaterials to meet the expanding technological demands;
- We have confirmed that the Nb₂C MXenes were a suitable additive for the SnO₂ ETL to make the PSCs work much better;
- Mechanisms that improve the performance of MXenes in solar cells are reviewed in depth for their future development and commercial use;
- Small Mxene (CoS) nanoparticles boost photovoltaic performance by generating excellent permeability, abundant catalytic active sites, ion-diffusion performance, and outstanding charge transfer.

Supplementary Materials: The following supporting information can be downloaded at: <https://www.mdpi.com/article/10.3390/nano12203666/s1>, Table S1: Summary of the key parameters for the solar cells employing MXenes; Table S2: Summary of the key parameters for the solar cells employing metal oxide; Table S3: Summary of the key parameters for the solar cells employing noble metals.

Author Contributions: Data curation, T.F.A.; funding acquisition, D.W.J.; resources, R.S. and A.N.; supervision, M.A.A.H. and W.Z.W.H.; writing—original draft, T.F.A. All authors have read and agreed to the published version of the manuscript.

Funding: This research was funded by the following research grants; Universiti Putra Malaysia (UPM) Research Grant (UPM/GP-IPB/2020/9688700), Jeju National University, and Korea Institute of Energy Technology Evaluation and Planning (KETEP) grant funded by the Korea government (MOTIE) (20206310100050, A development of remanufacturing technology on the grinding system of complex-function for high-precision).

Institutional Review Board Statement: Not applicable.

Informed Consent Statement: Not applicable.

Acknowledgments: The authors would like to acknowledge Universiti Putra Malaysia (UPM), University of Malaya, Jeju National University, Korea Institute of Energy Technology Evaluation and Planning (KETEP), and Sunway University for providing the necessary resources for this publication.

Conflicts of Interest: The authors declare no conflict of interest.

References

1. Da, Y.; Xuan, Y.; Li, Q. From light trapping to solar energy utilization: A novel photovoltaic–thermoelectric hybrid system to fully utilize solar spectrum. *Energy* **2016**, *95*, 200–210. [[CrossRef](#)]
2. Tyagi, V.V.; Rahim, N.A.A.; Rahim, N.A.; Selvaraj, J.A.L. Progress in solar PV technology: Research and achievement. *Renew. Sustain. Energy Rev.* **2013**, *20*, 443–461. [[CrossRef](#)]
3. Husain, A.A.F.; Hasan, W.Z.W.; Shafie, S.; Hamidon, M.N.; Pandey, S.S. A review of transparent solar photovoltaic technologies. *Renew. Sustain. Energy Rev.* **2018**, *94*, 779–791. [[CrossRef](#)]
4. Mancini, F.; Nastasi, B.; Mancini, F.; Nastasi, B. Solar Energy Data Analytics: PV Deployment and Land Use. *Energies* **2020**, *13*, 417. [[CrossRef](#)]
5. Ali, O.M.; Alomar, O.R. Technical and economic feasibility analysis of a PV grid-connected system installed on a university campus in Iraq. *Environ. Sci. Pollut. Res.* **2022**, *29*, 1–13. [[CrossRef](#)]
6. Noh, J.H.; Im, S.H.; Heo, J.H.; Mandal, T.N.; Seok, S. II Chemical management for colorful, efficient, and stable inorganic-organic hybrid nanostructured solar cells. *Nano Lett.* **2013**, *13*, 1764–1769. [[CrossRef](#)]
7. Xing, G.; Mathews, N.; Sun, S.; Lim, S.S.; Lam, Y.M.; Graetzel, M.; Mhaisalkar, S.; Sum, T.C. Long-range balanced electron-and hole-transport lengths in organic-inorganic CH₃NH₃PbI₃. *Science* **2013**, *342*, 344–347. [[CrossRef](#)]
8. Kumar, B.A.; Vetrivelan, V.; Ramalingam, G.; Manikandan, A.; Viswanathan, S.; Boomi, P.; Ravi, G. Computational studies and experimental fabrication of DSSC device assembly on 2D-layered TiO₂ and MoS₂@TiO₂ nanomaterials. *Phys. B Condens. Matter* **2022**, *633*, 413770. [[CrossRef](#)]
9. Naguib, M.; Kurtoglu, M.; Presser, V.; Lu, J.; Niu, J.; Heon, M.; Hultman, L.; Gogotsi, Y.; Barsoum, M.W. Two-Dimensional Nanocrystals Produced by Exfoliation of Ti₃AlC₂. *Adv. Mater.* **2011**, *37*, 4248–4253. [[CrossRef](#)]
10. Gao, F.; Zhao, Y.; Zhang, X.; You, J. Recent Progresses on Defect Passivation toward Efficient Perovskite Solar Cells. *Adv. Energy Mater.* **2020**, *10*, 1902650. [[CrossRef](#)]

11. Han, T.-H.; Tan, S.; Xue, J.; Meng, L.; Lee, J.-W.; Yang, Y.; Han, T.; Tan, S.; Xue, J.; Meng, L.; et al. Interface and Defect Engineering for Metal Halide Perovskite Optoelectronic Devices. *Adv. Mater.* **2019**, *31*, e1803515. [[CrossRef](#)] [[PubMed](#)]
12. Guo, Z.; Gao, L.; Xu, Z.; Teo, S.; Zhang, C.; Kamata, Y.; Hayase, S.; Ma, T.; Guo, Z.; Xu, Z.; et al. High Electrical Conductivity 2D MXene Serves as Additive of Perovskite for Efficient Solar Cells. *Small* **2018**, *14*, e1802738. [[CrossRef](#)] [[PubMed](#)]
13. Agresti, A.; Pazniak, A.; Pescetelli, S.; Di Vito, A.; Rossi, D.; Pecchia, A.; Auf der Maur, M.; Liedl, A.; Larciprete, R.; Kuznetsov, D.V.; et al. Titanium-carbide MXenes for work function and interface engineering in perovskite solar cells. *Nat. Mater.* **2019**, *18*, 1228–1234. [[CrossRef](#)]
14. Bati, A.; Sutanto, A.A.; Hao, M.; Batmunkh, M. Cesium-doped Ti₃C₂T_x MXene for efficient and thermally stable perovskite solar cells. *Cell Rep. Phys. Sci.* **2021**, *2*, 100598. [[CrossRef](#)]
15. Alhamada, T.F.; Azmah Hanim, M.A.; Jung, D.W.; Nuraini, A.A.; Wan Hasan, W.Z. A brief review of the role of 2D mxene nanosheets toward solar cells efficiency improvement. *Nanomaterials* **2021**, *11*, 2732. [[CrossRef](#)] [[PubMed](#)]
16. McDaniel, R.M.; Carey, M.S.; Wilson, O.R.; Barsoum, M.W.; Magenau, A.J.D. Well-Dispersed Nanocomposites Using Covalently Modified, Multilayer, 2D Titanium Carbide (MXene) and In-Situ “click” Polymerization. *Chem. Mater.* **2021**, *33*, 1648–1656. [[CrossRef](#)]
17. Karomah, B.A. MXene Nanomaterials for Future Solar Energy Technologies Solar Cell using MXene and other Beneficial. *Nanomaterials* **2021**, 1–5.
18. Liu, M.; Johnston, M.B.; Snaith, H.J. Efficient planar heterojunction perovskite solar cells by vapour deposition. *Nature* **2013**, *501*, 395–398. [[CrossRef](#)]
19. Li, R.; Zhang, L.; Shi, L.; Wang, P. MXene Ti₃C₂: An Effective 2D Light-to-Heat Conversion Material. *ACS Nano* **2017**, *11*, 3752–3759. [[CrossRef](#)]
20. Pang, J.; Mendes, R.G.; Bachmatiuk, A.; Zhao, L.; Ta, H.Q.; Gemming, T.; Liu, H.; Liu, Z.; Rummeli, M.H. Applications of 2D MXenes in energy conversion and storage systems. *Chem. Soc. Rev.* **2019**, *48*, 72–133. [[CrossRef](#)]
21. Chen, T.; Tong, G.; Xu, E.; Li, H.; Li, P.; Zhu, Z.; Tang, J.; Qi, Y.; Jiang, Y. Accelerating hole extraction by inserting 2D Ti₃C₂-MXene interlayer to all inorganic perovskite solar cells with long-term stability. *J. Mater. Chem. A* **2019**, *7*, 20597–20603. [[CrossRef](#)]
22. Jaya Prakash, N.; Kandasubramanian, B. Nanocomposites of MXene for industrial applications. *J. Alloys Compd.* **2021**, *862*, 158547. [[CrossRef](#)]
23. Asgharizadeh, S.; Khesali Azadi, S. Additive MXene and dominant recombination channel in perovskite solar cells. *Sol. Energy* **2022**, *241*, 720–727. [[CrossRef](#)]
24. Niu, Y.; Tian, C.; Gao, J.; Fan, F.; Zhang, Y.; Mi, Y.; Ouyang, X.; Li, L.; Li, J.; Chen, S.; et al. Nb₂C MXenes modified SnO₂ as high quality electron transfer layer for efficient and stability perovskite solar cells. *Nano Energy* **2021**, *89*, 106455. [[CrossRef](#)]
25. Liu, D.; Traverse, C.J.; Chen, P.; Elinski, M.; Yang, C.; Wang, L.; Young, M.; Lunt, R.R.; Liu, D.; Traverse, C.J.; et al. Aqueous-Containing Precursor Solutions for Efficient Perovskite Solar Cells. *Adv. Sci.* **2018**, *5*, 1700484. [[CrossRef](#)] [[PubMed](#)]
26. Zhao, D.; Chen, C.; Wang, C.; Junda, M.M.; Song, Z.; Grice, C.R.; Yu, Y.; Li, C.; Subedi, B.; Podraza, N.J.; et al. Efficient two-terminal all-perovskite tandem solar cells enabled by high-quality low-bandgap absorber layers. *Nat. Energy* **2018**, *3*, 1093–1100. [[CrossRef](#)]
27. Tong, J.; Song, Z.; Kim, D.H.; Chen, X.; Chen, C.; Palmstrom, A.F.; Ndione, P.F.; Reese, M.O.; Dunfield, S.P.; Reid, O.G.; et al. Carrier lifetimes of >1 ms in Sn-Pb perovskites enable efficient all-perovskite tandem solar cells. *Science* **2019**, *364*, 475–479. [[CrossRef](#)] [[PubMed](#)]
28. Jung, E.H.; Jeon, N.J.; Park, E.Y.; Moon, C.S.; Shin, T.J.; Yang, T.Y.; Noh, J.H.; Seo, J. Efficient, stable and scalable perovskite solar cells using poly(3-hexylthiophene). *Nature* **2019**, *567*, 511–515. [[CrossRef](#)] [[PubMed](#)]
29. Jin, X.; Yang, L.; Wang, X.F. Efficient Two-Dimensional Perovskite Solar Cells Realized by Incorporation of Ti₃C₂T_x MXene as Nano-Dopants. *Nano-Micro Lett.* **2021**, *13*, 68. [[CrossRef](#)] [[PubMed](#)]
30. Shi, Z.; Khaledialidusti, R.; Malaki, M. MXene-Based Materials for Solar Cell Applications. *Nanomaterials* **2021**, *11*, 3170. [[CrossRef](#)] [[PubMed](#)]
31. Zhang, Z.; Li, Y.; Liang, C.; Yu, G.; Zhao, J.; Luo, S.; Huang, Y.; Su, C.; Xing, G.; Zhang, Z.P.; et al. In Situ Growth of MAPbBr₃ Nanocrystals on Few-Layer MXene Nanosheets with Efficient Energy Transfer. *Small* **2020**, *16*, e1905896. [[CrossRef](#)] [[PubMed](#)]
32. Gao, L.; Li, C.; Huang, W.; Mei, S.; Lin, H.; Ou, Q.; Zhang, Y.; Guo, J.; Zhang, F.; Xu, S.; et al. MXene/Polymer Membranes: Synthesis, Properties, and Emerging Applications. *Chem. Mater.* **2020**, *32*, 1703–1747. [[CrossRef](#)]
33. Abraham, B.M.; Parey, V.; Singh, J.K. A strategic review of MXenes as emergent building blocks for future two-dimensional materials: Recent progress and perspectives. *J. Mater. Chem. C* **2022**, *10*, 4096–4123. [[CrossRef](#)]
34. Xu, H.; Yin, X.; Li, X.; Li, M.; Liang, S.; Zhang, L.; Cheng, L. Lightweight Ti₂CT_x MXene/Poly(vinyl alcohol) Composite Foams for Electromagnetic Wave Shielding with Absorption-Dominated Feature. *ACS Appl. Mater. Interfaces* **2019**, *11*, 10198–10207. [[CrossRef](#)]
35. Cao, Y.; Deng, Q.; Liu, Z.; Shen, D.; Wang, T.; Huang, Q.; Du, S.; Jiang, N.; Lin, C.T.; Yu, J. Enhanced thermal properties of poly(vinylidene fluoride) composites with ultrathin nanosheets of MXene. *RSC Adv.* **2017**, *7*, 20494–20501. [[CrossRef](#)]
36. Han, R.; Ma, X.; Xie, Y.; Teng, D.; Zhang, S. Preparation of a new 2D MXene/PES composite membrane with excellent hydrophilicity and high flux. *RSC Adv.* **2017**, *7*, 56204–56210. [[CrossRef](#)]
37. Si, J.Y.; Tawiah, B.; Sun, W.L.; Lin, B.; Wang, C.; Yuen, A.C.Y.; Yu, B.; Li, A.; Yang, W.; Lu, H.D.; et al. Functionalization of MXene Nanosheets for Polystyrene towards High Thermal Stability and Flame Retardant Properties. *Polymers* **2019**, *11*, 976. [[CrossRef](#)]

38. Yu, B.; Tawiah, B.; Wang, L.Q.; Yin Yuen, A.C.; Zhang, Z.C.; Shen, L.L.; Lin, B.; Fei, B.; Yang, W.; Li, A.; et al. Interface decoration of exfoliated MXene ultra-thin nanosheets for fire and smoke suppressions of thermoplastic polyurethane elastomer. *J. Hazard. Mater.* **2019**, *374*, 110–119. [CrossRef]
39. Malaki, M.; Varma, R.S. Mechanotribological Aspects of MXene-Reinforced Nanocomposites. *Adv. Mater.* **2020**, *32*, 2003154. [CrossRef]
40. Naguib, M.; Saito, T.; Lai, S.; Rager, M.S.; Aytug, T.; Parans Paranthaman, M.; Zhao, M.Q.; Gogotsi, Y. $Ti_3C_2T_x$ (MXene)-polyacrylamide nanocomposite films. *RSC Adv.* **2016**, *6*, 72069–72073. [CrossRef]
41. Deng, D.; Guo, H.; Ji, B.; Wang, W.; Ma, L.; Luo, F. Size-selective catalysts in five functionalized porous coordination polymers with unsaturated zinc centers. *New J. Chem.* **2017**, *41*, 12611–12616. [CrossRef]
42. Chang, X.H.; Qin, W.J.; Zhang, X.Y.; Jin, X.; Yang, X.G.; Dou, C.X.; Ma, L.F. Angle-Dependent Polarized Emission and Photoelectron Performance of Dye-Encapsulated Metal-Organic Framework. *Inorg. Chem.* **2021**, *60*, 10109–10113. [CrossRef] [PubMed]
43. Chang, X.H. Synthesis and structure of a zinc(II) coordination polymer assembled with 5-(3-carboxybenzyloxy)isophthalic acid and 1,2-bis(4-pyridyl)ethane. *Zeitschrift fur Naturforsch. Sect. B J. Chem. Sci.* **2022**, *77*, 561–564. [CrossRef]
44. Li, J.X.; Zhang, Y.H.; Du, Z.X.; Feng, X. One-pot solvothermal synthesis of mononuclear and oxalate-bridged binuclear nickel compounds: Structural analyses, conformation alteration and magnetic properties. *Inorganica Chim. Acta* **2022**, *530*, 120697. [CrossRef]
45. Li, J.X.; Xiong, L.Y.; Fu, L.L.; Bo, W.B.; Du, Z.X.; Feng, X. Structural diversity of Mn(II) and Cu(II) complexes based on 2-carboxyphenoxyacetate linker: Syntheses, conformation comparison and magnetic properties. *J. Solid State Chem.* **2022**, *305*, 122636. [CrossRef]
46. Yang, R.; Chen, X.; Ke, W.; Wu, X. Recent Research Progress in the Structure, Fabrication, and Application of MXene-Based Heterostructures. *Nanomaterials* **2022**, *12*, 1907. [CrossRef]
47. Tariq, A.; Iqbal, M.A.; Ali, S.I.; Iqbal, M.Z.; Akinwande, D.; Rizwan, S. Ti_3C_2 -MXene/Bismuth Ferrite Nanohybrids for Efficient Degradation of Organic Dye and Colorless Pollutant. *ACS Omega* **2019**, *4*, 20530–20539. [CrossRef]
48. Chen, X.; Li, J.; Pan, G.; Xu, W.; Zhu, J.; Zhou, D.; Li, D.; Chen, C.; Lu, G.; Song, H. Ti_3C_2 MXene quantum dots/ TiO_2 inverse opal heterojunction electrode platform for superior photoelectrochemical biosensing. *Sens. Actuators B Chem.* **2019**, *289*, 131–137. [CrossRef]
49. Zhang, H.; Li, M.; Zhu, C.; Tang, Q.; Kang, P.; Cao, J. Preparation of magnetic $\alpha-Fe_2O_3/ZnFe_2O_4@Ti_3C_2$ MXene with excellent photocatalytic performance. *Ceram. Int.* **2020**, *46*, 81–88. [CrossRef]
50. Chen, L.; Ye, X.; Chen, S.; Ma, L.; Wang, Z.; Wang, Q.; Hua, N.; Xiao, X.; Cai, S.; Liu, X. Ti_3C_2 MXene nanosheet/ TiO_2 composites for efficient visible light photocatalytic activity. *Ceram. Int.* **2020**, *46*, 25895–25904. [CrossRef]
51. Wang, Z.; Cheng, Z.; Xie, L.; Hou, X.; Fang, C. Flexible and lightweight $Ti_3C_2T_x$ MXene/ $Fe_3O_4@PANI$ composite films for high-performance electromagnetic interference shielding. *Ceram. Int.* **2021**, *47*, 5747–5757. [CrossRef]
52. Dele-Afolabi, T.T.; Mohamed Ariff, A.H.; Ojo-Kupoluyi, O.J.; Adefajo, A.A.; Oyewo, T.A.; Hashmi, S.; Saidur, R. *Processing Techniques and Application Areas of MXene-Reinforced Nanocomposites*; Elsevier Ltd.: Amsterdam, The Netherlands, 2021; ISBN 9780128203521.
53. Chen, X.; Zhuang, Y.; Shen, Q.; Cao, X.; Yang, W.; Yang, P. In situ synthesis of $Ti_3C_2T_x$ MXene/CoS nanocomposite as high performance counter electrode materials for quantum dot-sensitized solar cells. *Sol. Energy* **2021**, *226*, 236–244. [CrossRef]
54. Cai, C.; Wang, R.; Liu, S.; Yan, X.; Zhang, L.; Wang, M.; Tong, Q.; Jiao, T. Synthesis of self-assembled phytic acid-MXene nanocomposites via a facile hydrothermal approach with elevated dye adsorption capacities. *Colloids Surfaces A Physicochem. Eng. Asp.* **2020**, *589*, 124468. [CrossRef]
55. Wang, L.; Liu, Z.Q.; Li, S.F.; Yang, Y.F.; Misra, R.D.K.; Li, J.; Ye, D.; Cui, J.Y.; Gan, X.M.; Tian, Z.J. Few-layered Ti_3C_2 MXene-coated Ti-6Al-4V composite powder for high-performance Ti matrix composite. *Compos. Commun.* **2022**, *33*, 101238. [CrossRef]
56. Xiao, S.; Zhang, X.; Zhang, J.; Wu, S.; Wang, J.; Chen, J.S.; Li, T. Enhancing the lithium storage capabilities of TiO_2 nanoparticles using delaminated MXene supports. *Ceram. Int.* **2018**, *44*, 17660–17666. [CrossRef]
57. Hu, J.; Li, S.; Zhang, J.; Chang, Q.; Yu, W.; Zhou, Y. Mechanical properties and frictional resistance of Al composites reinforced with $Ti_3C_2T_x$ MXene. *Chin. Chem. Lett.* **2020**, *31*, 996–999. [CrossRef]
58. Mai, Y.J.; Li, Y.G.; Li, S.L.; Zhang, L.Y.; Liu, C.S.; Jie, X.H. Self-lubricating Ti_3C_2 nanosheets/copper composite coatings. *J. Alloys Compd.* **2019**, *770*, 1–5. [CrossRef]
59. Ali, A.; Hantanasirisakul, K.; Abdala, A.; Urbankowski, P.; Zhao, M.Q.; Anasori, B.; Gogotsi, Y.; Aïssa, B.; Mahmoud, K.A. Effect of Synthesis on Performance of MXene/Iron Oxide Anode Material for Lithium-Ion Batteries. *Langmuir* **2018**, *34*, 11325–11334. [CrossRef]
60. Lai, S.; Jeon, J.; Jang, S.K.; Xu, J.; Choi, Y.J.; Park, J.H.; Hwang, E.; Lee, S. Surface group modification and carrier transport properties of layered transition metal carbides (Ti_2CT_x , T: -OH, -F and -O). *Nanoscale* **2015**, *7*, 19390–19396. [CrossRef]
61. Sherryana, A.; Tahir, M. Role of surface morphology and terminating groups in titanium carbide MXenes ($Ti_3C_2T_x$) cocatalysts with engineering aspects for modulating solar hydrogen production: A critical review. *Chem. Eng. J.* **2022**, *433*, 134573. [CrossRef]
62. Khazaei, M.; Arai, M.; Sasaki, T.; Chung, C.Y.; Venkataramanan, N.S.; Estili, M.; Sakka, Y.; Kawazoe, Y. Novel Electronic and Magnetic Properties of Two-Dimensional Transition Metal Carbides and Nitrides. *Adv. Funct. Mater.* **2013**, *23*, 2185–2192. [CrossRef]

63. Prasad, C.; Yang, X.; Liu, Q.; Tang, H.; Rammohan, A.; Zulfiqar, S.; Zyryanov, G.V.; Shah, S. Recent advances in MXenes supported semiconductors based photocatalysts: Properties, synthesis and photocatalytic applications. *J. Ind. Eng. Chem.* **2020**, *85*, 1–33. [[CrossRef](#)]
64. Enyashin, A.N.; Ivanovskii, A.L. Atomic structure, comparative stability and electronic properties of hydroxylated Ti_2C and Ti_3C_2 nanotubes. *Comput. Theor. Chem.* **2012**, *989*, 27–32. [[CrossRef](#)]
65. Schultz, T.; Frey, N.C.; Hantanasirisakul, K.; Park, S.; May, S.J.; Shenoy, V.B.; Gogotsi, Y.; Koch, N. Surface Termination Dependent Work Function and Electronic Properties of $Ti_3C_2T_x$ MXene. *Chem. Mater.* **2019**, *31*, 6590–6597. [[CrossRef](#)]
66. Sreedhar, A.; Noh, J.S. Recent advances in partially and completely derived 2D Ti_3C_2 MXene based TiO_2 nanocomposites towards photocatalytic applications: A review. *Sol. Energy* **2020**, *222*, 48–73. [[CrossRef](#)]
67. Guo, J.; Legum, B.; Anasori, B.; Wang, K.; Lelyukh, P.; Gogotsi, Y.; Randall, C.A.; Guo, J.; Wang, K.; Randall, C.A.; et al. Cold Sintered Ceramic Nanocomposites of 2D MXene and Zinc Oxide. *Adv. Mater.* **2018**, *30*, e1801846. [[CrossRef](#)] [[PubMed](#)]
68. Wozniak, J.; Petrus, M.; Cygan, T.; Jastrzebska, A.; Wojciechowski, T.; Ziemkowska, W.; Olszyna, A. Silicon carbide matrix composites reinforced with two-dimensional titanium carbide—Manufacturing and properties. *Ceram. Int.* **2019**, *45*, 6624–6631. [[CrossRef](#)]
69. Kannan, K.; Sliem, M.H.; Abdullah, A.M.; Sadasivuni, K.K.; Kumar, B. Fabrication of ZnO-Fe-MXene Based Nanocomposites for Efficient CO₂ Reduction. *Catalyst* **2020**, *10*, 549. [[CrossRef](#)]
70. Malaki, M.; Xu, W.; Kasar, A.K.; Menezes, P.L.; Dieringa, H.; Varma, R.S.; Gupta, M. Advanced Metal Matrix Nanocomposites. *Metals* **2019**, *9*, 330. [[CrossRef](#)]
71. Zheng, Z.; Liu, H.; Wu, D.; Wang, X. Polyimide/MXene hybrid aerogel-based phase-change composites for solar-driven seawater desalination. *Chem. Eng. J.* **2022**, *440*, 135862. [[CrossRef](#)]
72. Hong Ng, V.M.; Huang, H.; Zhou, K.; Lee, P.S.; Que, W.; Xu, J.Z.; Kong, L.B. Recent progress in layered transition metal carbides and/or nitrides (MXenes) and their composites: Synthesis and applications. *J. Mater. Chem. A* **2017**, *5*, 3039–3068. [[CrossRef](#)]
73. Anasori, B.; Lukatskaya, M.R.; Gogotsi, Y. 2D metal carbides and nitrides (MXenes) for energy storage. *Nat. Rev. Mater.* **2017**, *2*, 16098. [[CrossRef](#)]
74. Chen, X.; Zhao, Y.; Li, L.; Wang, Y.; Wang, J.; Xiong, J.; Du, S.; Zhang, P.; Shi, X.; Yu, J. MXene/Polymer Nanocomposites: Preparation, Properties, and Applications. *Polym. Rev.* **2020**, *61*, 80–115. [[CrossRef](#)]
75. Huang, Z.; Wang, S.; Kota, S.; Pan, Q.; Barsoum, M.W.; Li, C.Y. Structure and crystallization behavior of poly(ethylene oxide)/ $Ti_3C_2T_x$ MXene nanocomposites. *Polymer* **2016**, *102*, 119–126. [[CrossRef](#)]
76. Sobolciak, P.; Ali, A.; Hassan, M.K.; Helal, M.I.; Tanvir, A.; Popelka, A.; Al-Maadeed, M.A.; Krupa, I.; Mahmoud, K.A. 2D $Ti_3C_2T_x$ (MXene)-reinforced polyvinyl alcohol (PVA) nanofibers with enhanced mechanical and electrical properties. *PLoS ONE* **2017**, *12*, e0183705. [[CrossRef](#)] [[PubMed](#)]
77. Liu, Y.; Zhang, J.; Zhang, X.; Li, Y.; Wang, J. $Ti_3C_2T_x$ Filler Effect on the Proton Conduction Property of Polymer Electrolyte Membrane. *ACS Appl. Mater. Interfaces* **2016**, *8*, 20352–20363. [[CrossRef](#)] [[PubMed](#)]
78. Lipatov, A.; Lu, H.; Alhabeab, M.; Anasori, B.; Gruverman, A.; Gogotsi, Y.; Sinitiskii, A. Elastic properties of 2D $Ti_3C_2T_x$ MXene monolayers and bilayers. *Sci. Adv.* **2018**, *4*, eaat0491. [[CrossRef](#)]
79. Ronchi, R.M.; Arantes, J.T.; Santos, S.F. Synthesis, structure, properties and applications of MXenes: Current status and perspectives. *Ceram. Int.* **2019**, *45*, 18167–18188. [[CrossRef](#)]
80. Sheng, X.; Zhao, Y.; Zhang, L.; Lu, X. Properties of two-dimensional Ti_3C_2 MXene/thermoplastic polyurethane nanocomposites with effective reinforcement via melt blending. *Compos. Sci. Technol.* **2019**, *181*, 107710. [[CrossRef](#)]
81. Chen, K.; Chen, Y.; Deng, Q.; Jeong, S.H.; Jang, T.S.; Du, S.; Kim, H.E.; Huang, Q.; Han, C.M. Strong and biocompatible poly(lactic acid) membrane enhanced by $Ti_3C_2T_z$ (MXene) nanosheets for Guided bone regeneration. *Mater. Lett.* **2018**, *229*, 114–117. [[CrossRef](#)]
82. Ling, Z.; Ren, C.E.; Zhao, M.Q.; Yang, J.; Giammarco, J.M.; Qiu, J.; Barsoum, M.W.; Gogotsi, Y. Flexible and conductive MXene films and nanocomposites with high capacitance. *Proc. Natl. Acad. Sci. USA* **2014**, *111*, 16676–16681. [[CrossRef](#)] [[PubMed](#)]
83. Carey, M.; Hinton, Z.; Sokol, M.; Alvarez, N.J.; Barsoum, M.W. Nylon-6/ $Ti_3C_2T_z$ MXene Nanocomposites Synthesized by in Situ Ring Opening Polymerization of ϵ -Caprolactam and Their Water Transport Properties. *ACS Appl. Mater. Interfaces* **2019**, *11*, 20425–20436. [[CrossRef](#)] [[PubMed](#)]
84. Hu, C.; Shen, F.; Zhu, D.; Zhang, H.; Xue, J.; Han, X. Characteristics of Ti_3C_2X -Chitosan Films with Enhanced Mechanical Properties. *Front. Energy Res.* **2017**, *4*, 41. [[CrossRef](#)]
85. Bati, A.S.R.; Hao, M.; Macdonald, T.J.; Batmunkh, M.; Yamauchi, Y.; Wang, L.; Shapter, J.G. 1D-2D Synergistic MXene-Nanotubes Hybrids for Efficient Perovskite Solar Cells. *Small* **2021**, *17*, 2101925. [[CrossRef](#)]
86. Yang, L.; Kan, D.; Dall’Agnese, C.; Dall’Agnese, Y.; Wang, B.; Jena, A.K.; Wei, Y.; Chen, G.; Wang, X.F.; Gogotsi, Y.; et al. Performance improvement of MXene-based perovskite solar cells upon property transition from metallic to semiconductive by oxidation of $Ti_3C_2T_x$ in air. *J. Mater. Chem. A* **2021**, *9*, 5016–5025. [[CrossRef](#)]
87. Yang, Y.; Lu, H.; Feng, S.; Yang, L.; Dong, H.; Wang, J.; Tian, C.; Li, L.; Lu, H.; Jeong, J.; et al. Modulation of perovskite crystallization processes towards highly efficient and stable perovskite solar cells with MXene quantum dot-modified SnO₂. *Energy Environ. Sci.* **2021**, *14*, 3447–3454. [[CrossRef](#)]
88. Zhao, Y.; Zhang, X.; Han, X.; Hou, C.; Wang, H.; Qi, J.; Li, Y.; Zhang, Q. Tuning the reactivity of PbI₂ film via monolayer $Ti_3C_2T_x$ MXene for two-step-processed CH₃NH₃PbI₃ solar cells. *Chem. Eng. J.* **2021**, *417*, 127912. [[CrossRef](#)]

89. Zhou, Q.; Duan, J.; Du, J.; Guo, Q.; Zhang, Q.; Yang, X.; Duan, Y.; Tang, Q. Tailored Lattice “Tape” to Confine Tensile Interface for 11.08%-Efficiency All-Inorganic CsPbBr₃ Perovskite Solar Cell with an Ultrahigh Voltage of 1.702 V. *Adv. Sci.* **2021**, *8*, 2101418. [[CrossRef](#)]
90. Yang, L.; Dall’Agnese, Y.; Hantanasirisakul, K.; Shuck, C.E.; Maleski, K.; Alhabeab, M.; Chen, G.; Gao, Y.; Sanehira, Y.; Jena, A.K.; et al. SnO₂-Ti₃C₂ MXene electron transport layers for perovskite solar cells. *J. Mater. Chem. A* **2019**, *7*, 5635–5642. [[CrossRef](#)]
91. Hou, C.; Yu, H. ZnO/Ti₃C₂Tx monolayer electron transport layers with enhanced conductivity for highly efficient inverted polymer solar cells. *Chem. Eng. J.* **2021**, *407*, 127192. [[CrossRef](#)]
92. Zhang, J.; Huang, C.; Yu, H. Modulate the work function of Nb₂CTx MXene as the hole transport layer for perovskite solar cells. *Appl. Phys. Lett.* **2021**, *119*, 033506. [[CrossRef](#)]
93. Xie, F.X.; Choy, W.C.H.; Sha, W.E.I.; Zhang, D.; Zhang, S.; Li, X.; Leung, C.W.; Hou, J. Enhanced charge extraction in organic solar cells through electron accumulation effects induced by metal nanoparticles. *Energy Environ. Sci.* **2013**, *6*, 3372–3379. [[CrossRef](#)]
94. Kogo, A.; Sanehira, Y.; Numata, Y.; Ikegami, M.; Miyasaka, T. Amorphous Metal Oxide Blocking Layers for Highly Efficient Low-Temperature Brookite TiO₂-Based Perovskite Solar Cells. *ACS Appl. Mater. Interfaces* **2018**, *10*, 2224–2229. [[CrossRef](#)]
95. Sharma, R.; Lee, H.; Borse, K.; Gupta, V.; Joshi, A.G.; Yoo, S.; Gupta, D. Ga-doped ZnO as an electron transport layer for PffBT4T-2OD: PC70BM organic solar cells. *Org. Electron.* **2017**, *43*, 207–213. [[CrossRef](#)]
96. Lin, C.Y.; Lai, Y.H.; Chen, H.W.; Chen, J.G.; Kung, C.W.; Vittal, R.; Ho, K.C. Highly efficient dye-sensitized solar cell with a ZnO nanosheet-based photoanode. *Energy Environ. Sci.* **2011**, *4*, 3448–3455. [[CrossRef](#)]
97. Baek, S.W.; Park, G.; Noh, J.; Cho, C.; Lee, C.H.; Seo, M.K.; Song, H.; Lee, J.Y. Au@Ag core-shell nanocubes for efficient plasmonic light scattering effect in low bandgap organic solar cells. *ACS Nano* **2014**, *8*, 3302–3312. [[CrossRef](#)] [[PubMed](#)]
98. Xu, X.; Kyaw, A.K.K.; Peng, B.; Xiong, Q.; Demir, H.V.; Wang, Y.; Wong, T.K.S.; Sun, X.W. Influence of gold-silica nanoparticles on the performance of small-molecule bulk heterojunction solar cells. *Org. Electron.* **2015**, *22*, 20–28. [[CrossRef](#)]
99. Baek, S.W.; Noh, J.; Lee, C.H.; Kim, B.; Seo, M.K.; Lee, J.Y. Plasmonic forward scattering effect in organic solar cells: A powerful optical engineering method. *Sci. Rep.* **2013**, *3*, 1726. [[CrossRef](#)]
100. Yao, K.; Salvador, M.; Chueh, C.C.; Xin, X.K.; Xu, Y.X.; Dequillettes, D.W.; Hu, T.; Chen, Y.; Ginger, D.S.; Jen, A.K.Y. A General Route to Enhance Polymer Solar Cell Performance using Plasmonic Nanoprisms. *Adv. Energy Mater.* **2014**, *4*, 1400206. [[CrossRef](#)]